Electronic Supplementary Information (ESI) for Chem. Commun.

A Helical Polypyrrole Nanotube interwoven Zeolitic Imidazolate Framework and Its Derivative as Oxygen Electrocatalysts

Zijia Bao,[a] Yanzhi Wang,[a] Mengke Shi,[a] Xinyue Wang,[a] Zuozhong Liang,[a] Zhehao Huang,[b] Wei Zhang,[a] Rui Cao,[a] Haoquan Zheng*[a]

[a]Key Laboratory of Applied Surface and Colloid Chemistry, Ministry of Education, School of Chemistry and Chemical Engineering, Shaanxi Normal University, Xi'an 710119, China.

[b]Department of Materials and Environmental Chemistry, Stockholm University, Stockholm SE-106 91, Sweden

Correspondence Email: zhenghaoquan@snnu.edu.cn

1. Experimental section

1.1 Materials

L-glutamic acid (L-Glu, 99%), acetone (99.7%), stearoyl chloride (98%), pyrrole (99%), ammonium persulfate (APS, 99%), $Co(NO)_3 \cdot 6H_2O$ (AR, 99%), 2-methylimidazole (AR, 99%), KOH (AR, 95%), $Zn(CH_3COO)_2 \cdot 2H_2O$ (AR, 99%) and ammonium persulfate (APS, 99%) were purchased from the Energy Chemical. NaOH (AR, 96%), HCl (36.0 ~ 38.0%), petroleum ether (AR), Methanol (AR, 99.5%) and Ethanol (AR, 99.7%) were purchased from Sinopharm Group Chemical Reagent Co., Ltd. All chemicals were used without further purification.

1.2 Preparation of chiral N-stearyl-glutamic acid (C_{18}-L-Glu)

Typically, 3.53 g of L-glutamic acid and 1.92 g of NaOH were dissolved in the mixed solution of 14 mL of deionized water (DIW) and 12 mL of acetone, keep the pH at 12. Then, 6.05 g of stearoyl chloride and 10 mL of NaOH solution (0.2 mol L^{-1}) were added slowly into the solution mentioned above and keep pH at 12 for 1 hour. Add HCl dropwise to the solution and adjust the pH=1 to obtain the carboxylic acid surfactant. Wash the obtained solid with DIW till pH=7. Then wash 5 times with the petroleum ether solvent and drying in the freeze dryer for 12 h to obtain C_{18}-L-Glu.

1.3 Synthesis of HPPy.

Typically, 0.0245 g of C_{18}-L-Glu was dissolved in 12.88 mL of methanol, stir 30 min to fully dissolve the surfactant. 166 μL pyrrole and 60 mL DIW were added into the above solution. After stirring 10 min, 1.2 mL of pre-cooled (0~5 °C) ammonium persulfate (APS) solution (containing 0.548 g APS) was added. Keep stirring 30 min, after filtrating and washing with DIW and ethanol, black solid named HPPy was obtained by drying at 60 °C in the oven for 12 h. CCNT was obtained by pyrolyzing HPPy at 900 °C for 3 h with the heating rate and cooling rate at 2 °C min^{-1} under Ar atmosphere.

1.4 Synthesis of Co-NCCN.

Firstly, 30 mg of HPPy was uniformly distributed in 30 mL of methanol by ultrasonic crusher. Then, 5 mL of methanol containing 1 mmol $Co(NO)_3 \cdot 6H_2O$ was added in the above solution. After stirring 10 min, 25 mL of methanol with 4 mmol 2-methylimidazole was poured into the above solution. After stirring 1 hour, the mixture was aging for 24 h. The obtained deep purple power was collected by the centrifugation (10000 rpm, 3 min) and washed with methanol for 3 times, named HPPy/ZIF. The 50 mg of HPPy/ZIF power was weighted and transfer to a quartz boat and carbonized in a tubular furnace under Ar atmosphere. Ar was blown 30 min before heating to remove the air in the tube, and heated at 900 °C for 3 h with the heating rate and cooling rate at 2 °C min^{-1}. The obtained black power was named Co-NCCN. Co-NC was synthesized by the same method without HPPy. Co-NC-2 was obtained with the same method, only

replaced the HPPy to the MWCNT. Physical mixture of HPPy and ZIF with the mass ratio of 1: 1 to obtain HPPy+ZIF, the HPPy+ZIF was pyrolyzing at the same condition to obtain Co-NC-3.

1.5 Characterization

The morphology of the materials was characterized on a scanning electron microscopy (SEM, Hitachi SU8020) at an accelerating voltage of 5 kV and a transmission electron microscope (TEM, JEOL JEM-2100) with a field emission gun operating at 200 kV. EDS analysis was conducted on an AMETEK Materials Analysis EDX equipped on the TEM. The diffuse reflectance circular dichroism (DR-CD) signals were collected with a JASCO J-1500 circular dichroism spectrophotometer. Powder X-ray diffraction (PXRD) patterns of the materials were obtained on an X-ray diffractometer (Bruker, D8 Advance, Cu *K*α, λ = 1.5406 Å, 40 kV/40 mA). Brunauer-Emmett-Teller (BET) specific surface area was measured in Micromeritics ASAP 2020. X-ray photoelectron spectroscopic (XPS) spectra were collected by a Kratos AXIS ULTRA XPS. The Raman spectra were measured with a Raman spectrometer (Renishaw, in Via Reflex).

1.6 Electrochemical measurement

All of electrochemical tests are conducted on the CHI 660E (CH Instruments) electrochemical workstation and a Pine Modulated Speed Rotator (Pine Research Instrumentation, Inc.) at 30 °C. All ORR and OER performance tests are evaluated by a three-electrode system. The counter electrode is a graphite rod, and the reference electrode is a saturated Ag/AgCl electrode.

The details of the ORR electrochemical tests are as follows: the working electrode is a rotating disk electrode (RDE) (5 mm, 0.196 cm^2) or a rotating ring disk electrode (RRDE) (5.61 mm, 0.247 cm^2). The catalyst ink is consisted of 2 mg catalyst, 10 μL of Nafion solution (5 wt%, DuPont), 333 μL of deionized water, and 166 μL of isopropanol. The mixture was ultrasonicated for about 1 h to prepare a homogeneous catalyst ink. Then, 20 μL catalyst ink was evenly dropped on the rotating disk electrode (RDE), the catalyst load is 0.08 mg. The cyclic voltammetry (CV) test is carried out in 0.1 M KOH filled with Ar or O_2 at the scan rate of 50 $mV \cdot s^{-1}$ after 15 cycles activation at the scan rate of 100 $mV \cdot s^{-1}$. The linear sweep voltammetry (LSV) tests are carried out in 0.1 M KOH O_2-saturated solution at a rotational speed range of 400 to 1600 rpm at the scan rate of 5 $mV \cdot s^{-1}$ after 100% IR compensation. The *j*-t chronoamperometric responses were measured at 0.664 V (versus to RHE). The electrochemical impedance spectroscopy (EIS) spectra were tested in 0.1 M KOH O_2-saturated solution at a rotational speed of 1600 rpm at 0.664 V (versus to RHE).

The details of the OER electrochemical tests are as follows, the working electrode is a glassy carbon (GC) electrode (3 mm, 0.07 cm^2). The catalyst ink is consisted of 2 mg catalyst, 10 μL of Nafion solution (5 wt%, DuPont), 333 μL of deionized water, and 166 μL of isopropanol. The mixture was ultrasonicated for about 1 h to prepare a homogeneous catalyst ink. Then, 6 μL ink was evenly dropped on the glassy carbon

(GC) electrode, the catalyst load is 0.024 mg. The LSV test is tested in 0.1 M KOH at the scan rate of 5 $mV \cdot s^{-1}$ after 100% IR compensation.

ORR measurement: The potentials corresponding to the reversible hydrogen electrode (RHE) electrode was calculated with the following equation:

$$E_{RHE} = E_{Ag/AgCl} + (0.197 + 0.0591 \times pH)$$

The number of electron transfers (n) tested with RDE is calculated by the Koutecky-Levich (K-L) formula:

$$\frac{1}{j} = \frac{1}{j_l} + \frac{1}{j_k} = \frac{1}{B\omega^{1/2}} + \frac{1}{j_k}$$

j is the measured current density; j_l is the diffusion current density; j_k is the dynamic current density; ω is the rotational speed (rpm); B can be confirmed by the Koutecky-Levich (K-L) formula:

$$B = 0.2nFC_0(D_0)^{2/3}\upsilon^{-1/6}$$

Where F is the Faraday constant (96485 C mol^{-1}); C_0 is the concentration of O_2 in 0.1 M KOH (1.2×10^{-6} mol cm^{-3}); D_0 is the diffusion coefficient of O_2 in 0.1 M KOH (1.9×10^{-5} cm^2 s^{-1}); υ is the viscosity of 0.1 M KOH (0.1 cm^2 s^{-1}).

The number of electron transfers (n) could also be calculated by the tests with RRDE by the following equation:

$$n = \frac{4I_d}{I_d + \frac{I_r}{N}}$$

where I_d is the disk current of RRDE; I_r is the ring current; and N is the ring current collection efficiency, which was determined to be ~ 0.37 with the LSV measurement in $K_3Fe[CN]_6$ solution. The yield percentage (H_2O_2%) can be calculated with the following equation:

$$H_2O_2\% = 200\frac{\frac{I_r}{N}}{I_d + \frac{I_r}{N}}$$

OER measurement: Calculate the potential corresponding to the reversible hydrogen electrode (RHE) electrode by the following formula:

$$E_{RHE} = E_{Ag/AgCl} + (0.197 + 0.059 \times pH)$$

The overpotential (η) is calculated by the following formula:

$$\eta = E_{RHE} - 1.23$$

Zn-air battery performance test: All zinc-air battery tests are performed on CHI 660E electrochemical workstation at room temperature. The battery consists of a

polished zinc foil with a diameter of 15 mm and a thickness of 0.25 mm as the anode, 6.0 M KOH and 0.2 M $Zn(OAc)_2$ $2H_2O$ electrolytes, and a carbon cloth/gas diffusion layer (CC/GDL) coated with catalyst as the cathode.

Preparation of the air cathode: The catalyst ink is consisted of 5 mg catalyst, 950 μL of ethanol, and 50 μL of Nafion aqueous solution (5 wt% DuPont). The mixture was ultrasonicated for about 1 h to prepare a homogeneous catalyst ink. Spread 450 μL of the catalyst ink dropwise on the carbon cloth/gas diffusion layer (CC/GDL). The load of the catalyst is about 2 mg cm^{-2}. The carbon cloth (1.5 cm × 1.5 cm) is attached to the gas diffusion layer (1.8 cm × 1.8 cm) by thermo-pressing.

The discharge characteristic curve is tested at a current density of 20 mA cm^{-2}. The long-term charge-discharge cycling curve was tested with flow cell at 2 mA cm^{-2}. Each of the charge and discharge cycle is consisted of 10 min charge process and 10 min discharge process, and the current density is 2 mA cm^{-2}. The dynamic charge and discharge polarization curves were tested by LSV at the scan rate of 10 mV s^{-1}.

Table S1. Electrochemical ORR activities and Zn-air battery performance of Co-based electrocatalysts in this work and other reported works.

ORR			Zn-air battery		
Catalyst	Electrolyte	$E_{1/2}$ vs RHE	Specific capacity (mAh g^{-1})@j (mA cm^{-2})	Open circuit voltage (V)	Ref.
Co-NCCN	**0.1M KOH**	**850 mV**	**797.6@20**	**1.50**	**This work**
Co-N_x-C	0.1M KOH	780 mV	749.4@20	1.44	*Adv. Mater.*, 2017, **29**, 1703185.[1]
3D Co/N-C	0.1M KOH	840 mV	--	--	*Chem. Eng. J.*, 2022, **433**, 134500.[2]
Co_4N	0.1M KOH	840 mV	794.1@10	1.46	*Energy Storage Mater.*, 2022, **46**, 553-562.[3]
NC-Co SA	0.1M KOH	870 mV	--	--	*ACS Catal.*, 2018, **8**, 8961-8969.[4]
Co_3O_{4-x}/NG	0.1M KOH	840 mV	700.6@10	1.49	*Appl. Catal. B*, 2020, **278**, 119300.[5]
BCN/rGO-Co	0.1M KOH	850 mV	765.0@10	1.46	*ACS Appl. Mater. Interfaces*, 2022, **14**, 17249-17258.[6]
Co/CoO@NSC	0.1M KOH	835 mV	759.7@10	1.51	*J. Energy Chem.*, 2022, **64**, 385-394[7]
CoZn-NC-700	0.1M KOH	840 mV	578.0@10	1.42	*Adv. Funct. Mater.*, 2017, **27**, 1700795.[8]
Co-NC-AD	0.1M KOH	860 mV	808.0@5	1.45	*J. Energy Chem.*, 2022, **70**, 211-218.[9]
$Co(OH)_2$/CoPt/N-CN	0.1M KOH	800 mV	682.0@20	--	*ACS Appl. Mater. Interfaces*, 2019, **11**, 4983-4994.[10]
Co@Co_3O_4@NC-900	0.1M KOH	800 mV	685.0@5	--	*J. Mater. Chem. A*, 2018, **6**, 1443-1453.[11]

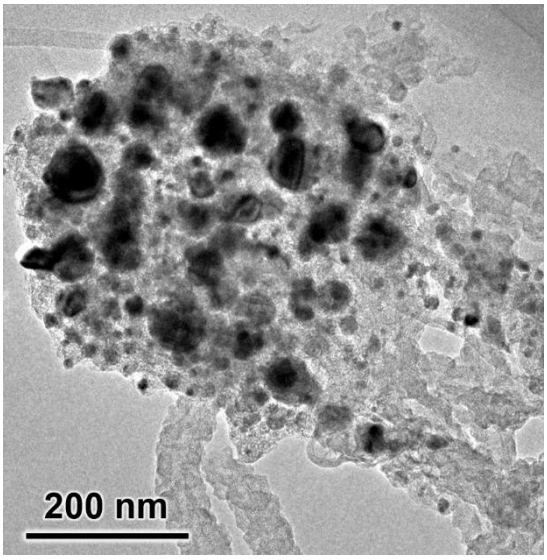

Fig. S1. TEM image of Co-NCCN.

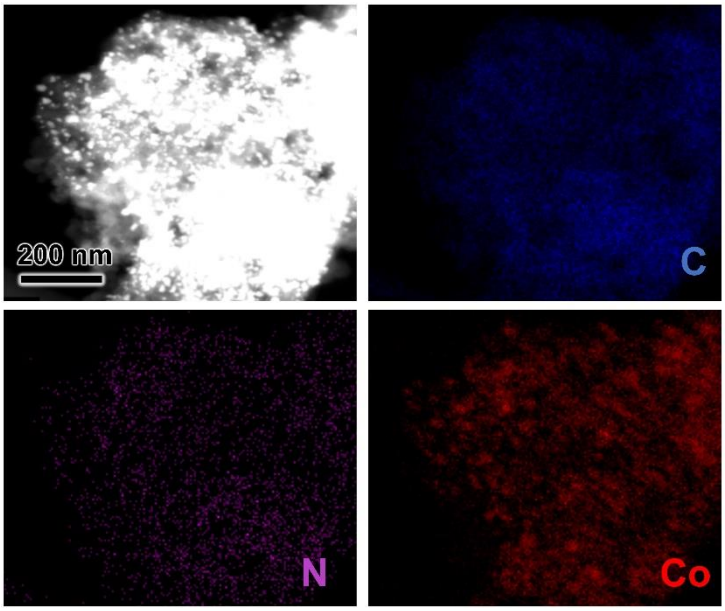

Fig. S2. The HAADF-STEM image and corresponding element mapping images of Co-NCCN.

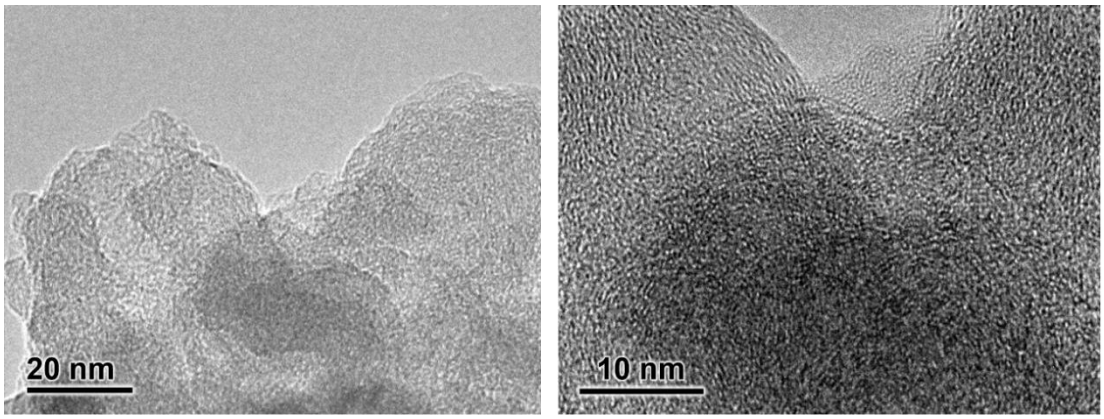

Fig. S3. TEM images of the interface of helical carbonaceous nanotubes and Co-NC derived from ZIF-67 in Co-NCCN.

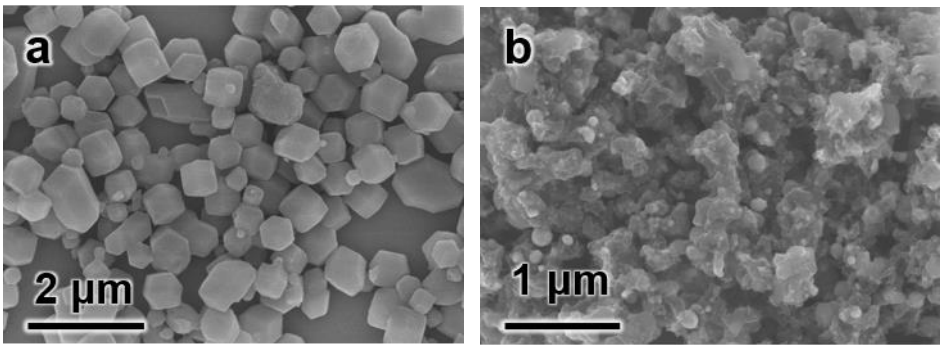

Fig. S4. SEM images of ZIF-67 (a) and Co-NC (b).

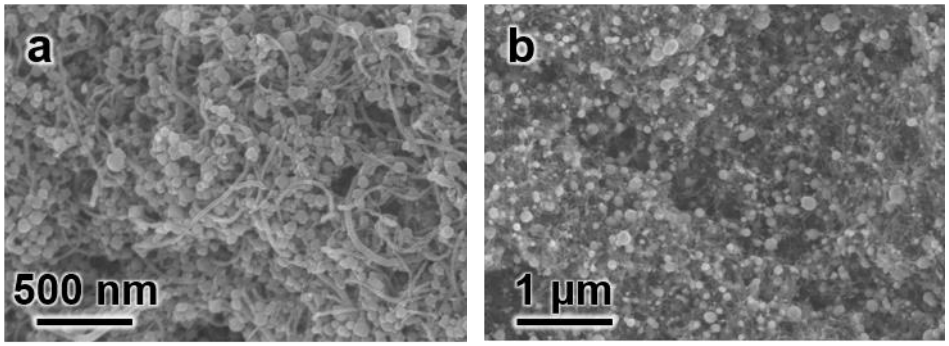

Fig. S5. SEM images of MWCNT/ZIF (a) and Co-NC-2 (b).

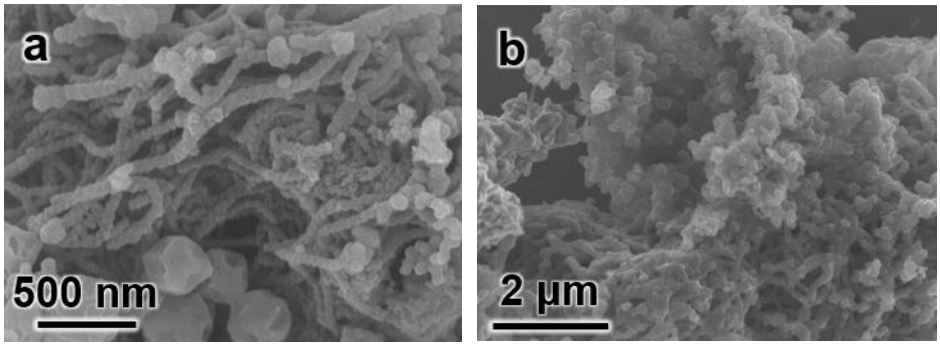

Fig. S6. SEM images of the physical mixture of HPPy+ZIF (a) and Co-NC-3 (b).

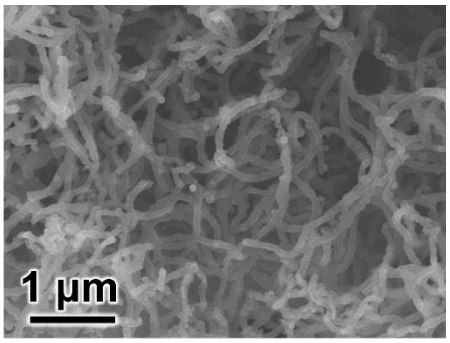

Fig. S7. SEM image of CCNT derived from HPPy.

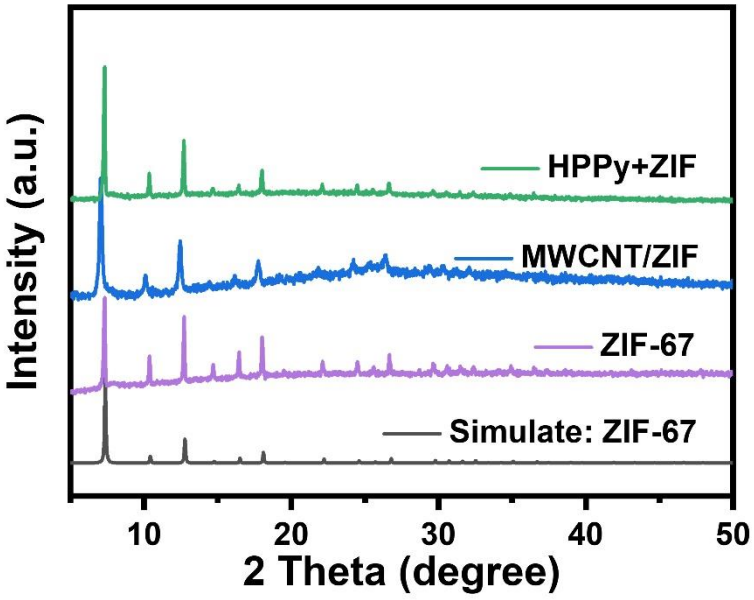

Fig. S8. PXRD of ZIF-67, MWCNT/ZIF, and HPPy+ZIF.

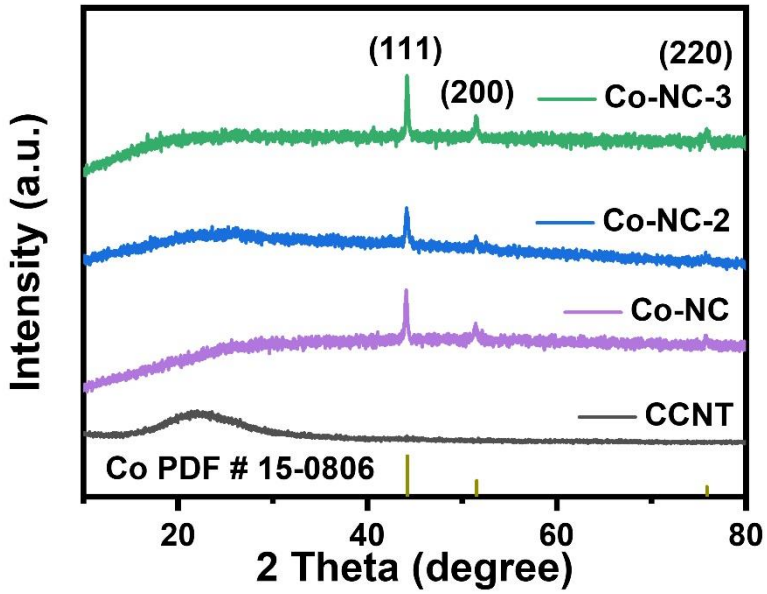

Fig. S9. PXRD of CCNT, Co-NC, Co-NC-2 and Co-NC-3.

After pyrolized at 900 °C under Ar atmosphere, the PXRD of the obtained Co-NC, Co-NC-2, and Co-NC-3 exhibit the diffraction peaks at 44.2°, 51.5° and 75.8°, which indexed to the {111}, {200} and {220} plants of Co (PDF#15-0806).

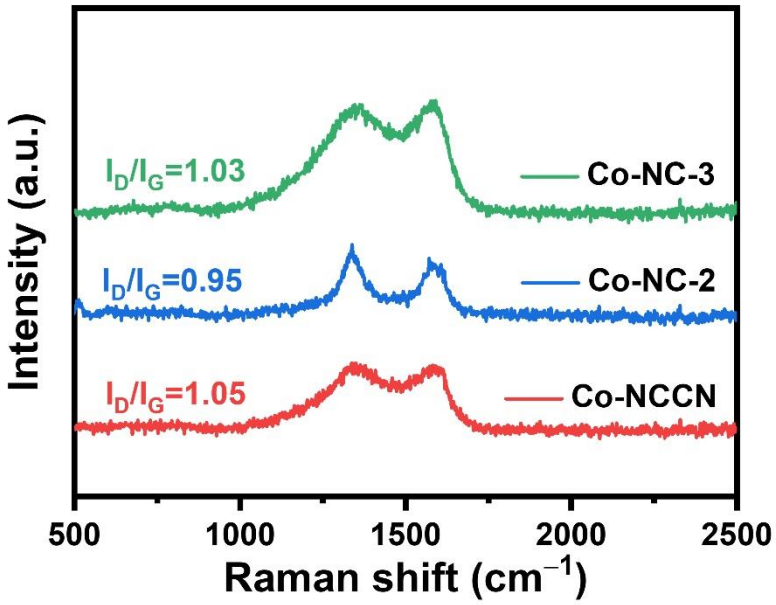

Fig. S10. Raman spectra of Co-NCCN, Co-NC-2, and Co-NC-3.

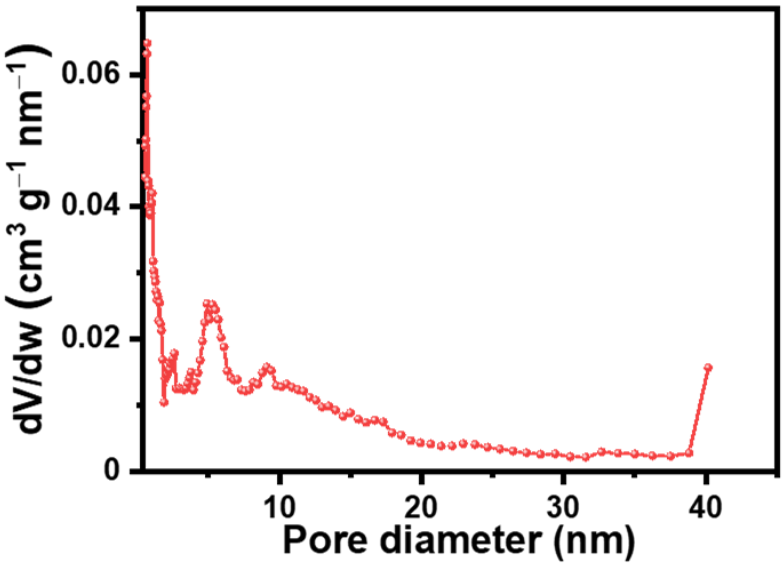

Fig. S11. The pore size distribution of Co-NCCN analyzed by the DFT model.

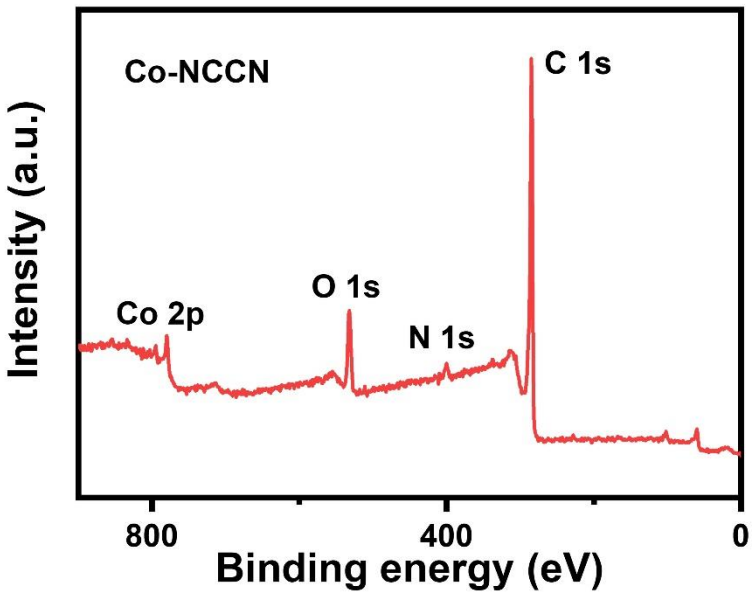

Fig. S12. XPS survey spectrum of Co-NCCN.

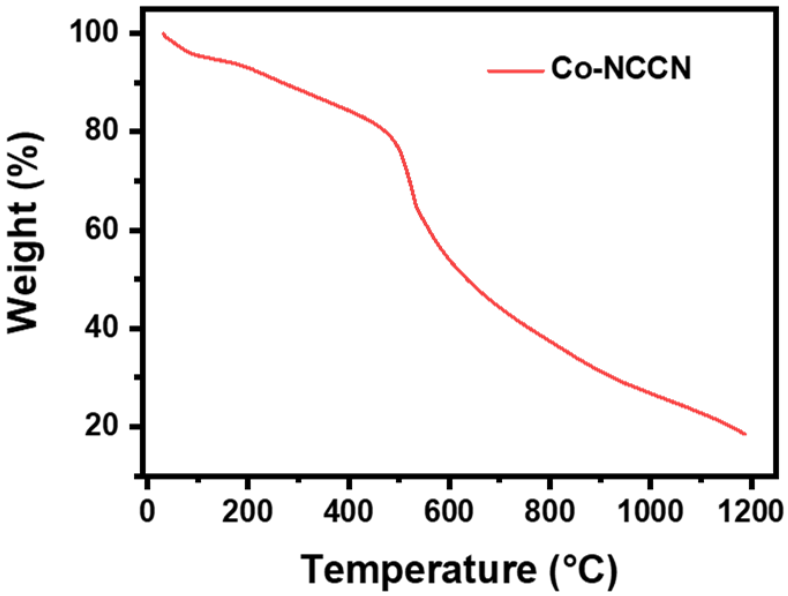

Fig. S13. Temperature dependent TGA of as-synthesized HPPy/ZIF-67 in Ar.

There is a weight loss of 20% below 500 ^{o}C due to the desorption of water and guest molecules. After reaching decomposition temperature of 500 ^{o}C, the weight loss was attributed to the collapse of the HPPy/ZIF-67 structure and carbonization under extreme thermal stress. After 700 ^{o}C, the weight loss is due to the transformation from defective carbon to graphitic carbon.

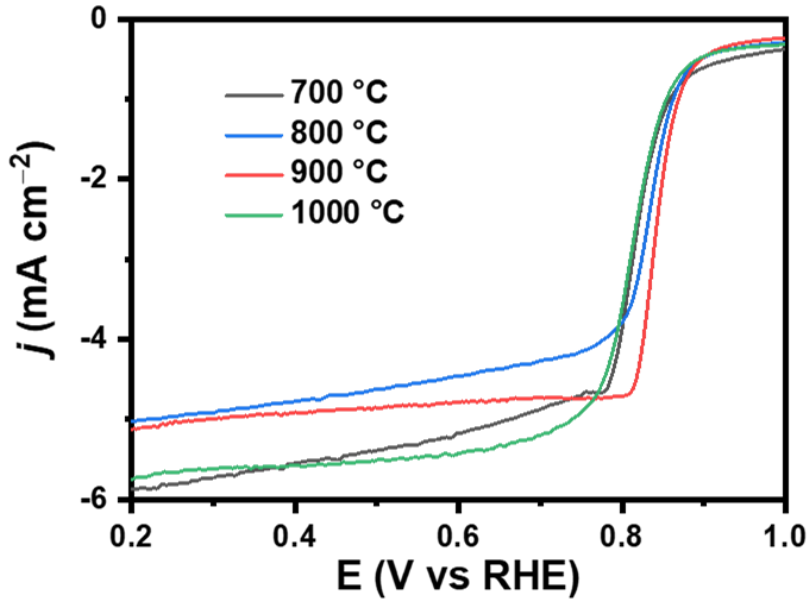

Fig. S14. LSV curves of Co-NCCN after calcined at different temperatures under Ar.

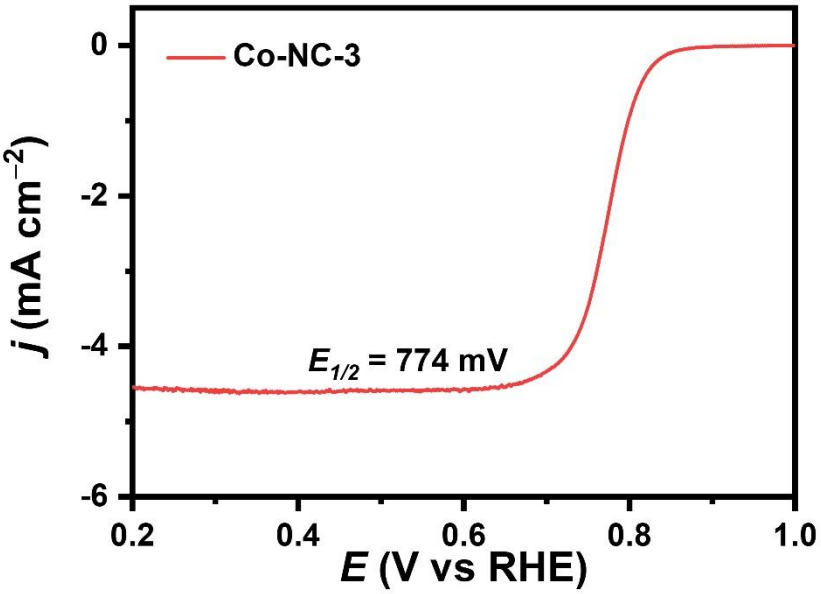

Fig. S15. LSV curve of Co-NC-3.

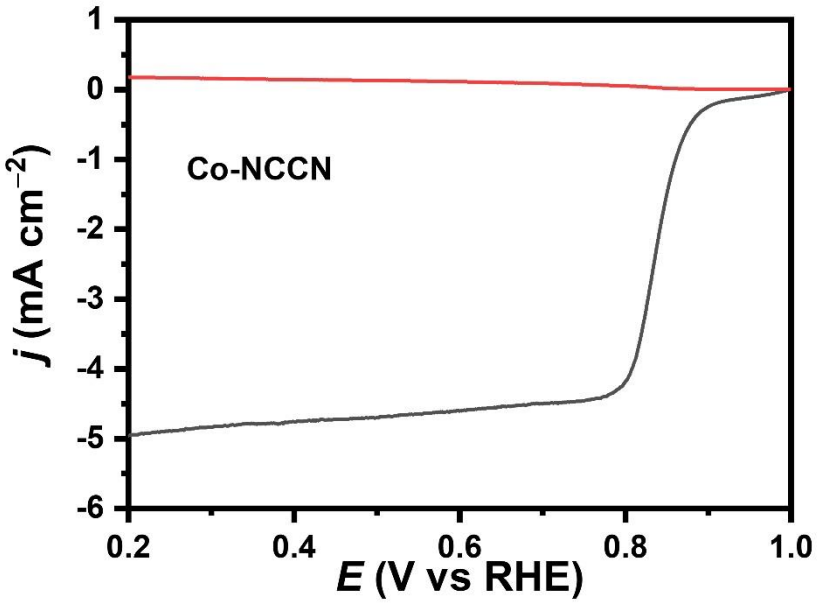

Fig. S16. LSV curves of Co-NCCN with RRDE.

LSV curves of Co-NCCN have been tested with rotating ring disk electrode (RRDE) in O_2-saturated 0.1 M KOH solution at 1600 rpm, the n of Co-NCCN is 3.74.

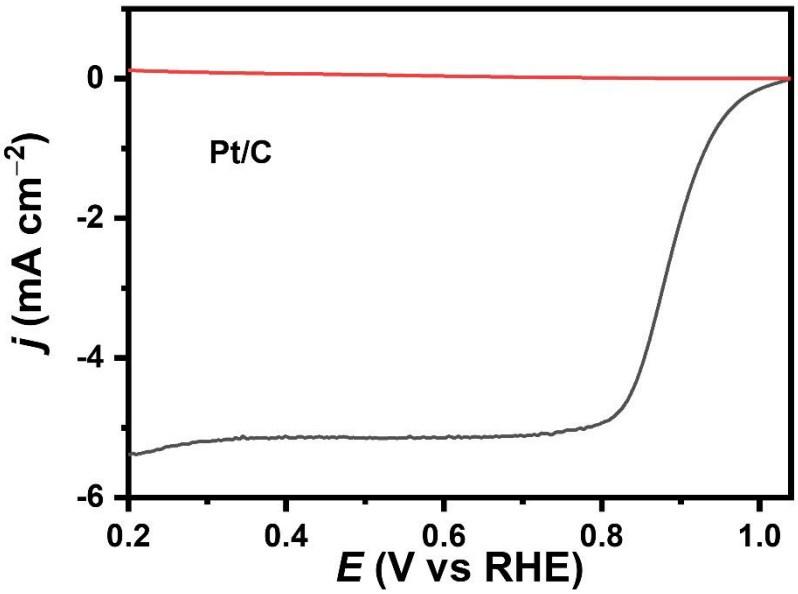

Fig. S17. LSV curves of commercial Pt/C with RRDE.

LSV curves of Co-NC Pt/C have been tested with RRDE in O_2-saturated 0.1 M KOH solution at 1600 rpm, the n of Pt/C is 3.9.

References:

1 C. Tang, B. Wang, H.F. Wang and Q. Zhang, *Adv. Mater.*, 2017, **29**, 1703185.
2 R. Wang, H. Yang, N. Lu, S. Lei, D. Jia, Z. Wang, Z. Liu, X. Wu, H. Zheng, S. Ali, F. Ma and S. Peng, *Chem. Eng. J.*, 2022, **433**, 134500.
3 H. Yang, S. Gao, D. Rao and X. Yan, *Energy Storage Mater.*, 2022, **46**, 553-562.
4 W. Zang, A. Sumboja, Y. Ma, H. Zhang, Y. Wu, S. Wu, H. Wu, Z. Liu, C. Guan, J. Wang and S.J. Pennycook, *ACS Catal.*, 2018, **8**, 8961-8969.
5 J. Qin, Z. Liu, D. Wu and J. Yang, *Appl. Catal. B*, 2020, **278**, 119300.
6 L. Cao, Y. Wang, Q. Zhu, L. Fan, Y. Wu, Z. Li, S. Xiong and F. Gu, *ACS Appl. Mater. Interfaces*, 2022, **14**, 17249-17258.
7 D. Zhou, H. Fu, J. Long, K. Shen and X. Gou, *J. Energy Chem.*, 2022, **64**, 385-394.
8 B. Chen, X. He, F. Yin, H. Wang, D.-J. Liu, R. Shi, J. Chen and H. Yin, *Adv. Funct. Mater.*, 2017, **27**, 1700795.
9 Y. Feng, K. Song, W. Zhang, X. Zhou, S.J. Yoo, J.-G. Kim, S. Qiao, Y. Qi, X. Zou, Z. Chen, T. Qin, N. Yue, Z. Wang, D. Li and W. Zheng, *J. Energy Chem.*, 2022, **70**, 211-218.
10 K. Wang, W. Wu, Z. Tang, L. Li, S. Chen and N.M. Bedford, *ACS Appl. Mater. Interfaces*, 2019, **11**, 4983-4994.
11 Z. Guo, F. Wang, Y. Xia, J. Li, A.G. Tamirat, Y. Liu, L. Wang, Y. Wang and Y. Xia, *J. Mater. Chem. A*, 2018, **6**, 1443-1453.